Available online at www.sciencedirect.com
ScienceDirect
Trans. Nonferrous Met. Soc. China 33(2023) 304−314
Transactions of Nonferrous Metals Society of China
www.tnmsc.cn

Leaching mechanism of strategic metals from superalloy scrap under ultrasonic cavitation

Long WANG[1], Yuan SUN[2,3], Shi-yang WANG[2,3], Ting-an ZHANG[1], Guo-zhi LÜ[1]

1. Key Laboratory for Ecological Utilization of Multimetallic Mineral, Ministry of Education, Northeastern University, Shenyang 110819, China;
2. Institute of Metal Research, Chinese Academy of Sciences, Shenyang 110016, China;
3. Joint Innovation Laboratory for Green Comprehensive Utilization of Superalloy Secondary Resources, Shenyang 110016, China

Received 17 October 2021; accepted 26 April 2022

Abstract: To improve the recovery efficiency of strategic metals from superalloy scrap, an ultrasonic-assisted leaching method was proposed. During the ultrasonic-assisted leaching process, at 60 min, the leaching rates of Re, Ni, Co, Al, Cr, and W are 92.3%, 95.2%, 98.5%, 98.7%, 97.5%, and 27.2%, respectively, which are far superior to those in the normal leaching process at 120 min. The improvement in leaching efficiency can be attributed to the physical and chemical coupling effects of ultrasonic cavitation. The physical effect can prevent the formation of the impeded dissolution layer and encourage contact between solution and superalloy scrap, which improves the leaching rates of strategic metals. The chemical effect can promote the production of hydroxyl radicals in the HCl−H_2O_2 system, which can enhance the potential of the leaching system, resulting in stimulation of the chemical oxidation process of Re to ReO_4^-.

Key words: strategic metals; superalloy scrap; leaching; ultrasonic-assisted leaching; hydroxyl radical

1 Introduction

Superalloys are frequently used as extreme structural components because of their excellent corrosion and mechanical properties at high temperatures [1]. In particular, Re, Ni, Co, Ta, and other strategic metals enhance corrosion and mechanical properties in a highly challenging environment [2,3]. However, considering the expensive current market value of strategic metals and the premium content of strategic metal in superalloy scrap, superalloy scrap is regarded as a desirable secondary source of strategic metals [4]. In addition, reasonable recovery of strategic metals from superalloy scrap can effectively alleviate the problem of insufficient strategic metal resources [5,6].

Owing to the outstanding physical and chemical performances [7−9], the recycling of superalloy scrap becomes quite burdensome [10,11]. One of the main drawbacks is the impeded dissolution layer on the surface of superalloy scrap, which consists of Al, Cr, Ta, W, and O [12−14]. The formation of the impeded dissolution layers prevents the superalloy from contacting the leaching solution and results in low recovery rates of strategic metals from superalloy scrap [15−17]. FENG et al [18] found that the inhibitory effect of chloride ions in the anode block dissolves layer

Corresponding author: Yuan SUN, Tel: +86-13840414962, E-mail: yuansun@imr.ac.cn;
Ting-an ZHANG, Tel: +86-13840205331, E-mail: zta2000@163.net
DOI: 10.1016/S1003-6326(22)66108-9

mainly embodied in the preferential adsorption of chloride ions on the working anode surface and the reduction of the combination of oxygen and metal cations. WANG et al [19] found that an organic electrolyte could promote the stripping of the impeded dissolution layers on the anode surface, effectively promoting the electrolytic reaction. FERNANDES et al [20] found that the electrolysis rate of various metals could be significantly enhanced by controlling the frequency and amplitude of alternating currents. However, the leaching rates of the strategic metals from superalloy scrap have not resulted in marked improvements.

Another drawback is the low recovery efficiency of rhenium caused by incomplete oxidation leaching reaction. Once reducing applied electric field intensity or oxidizer dosage, the oxidation reaction of rhenium in the leaching solution is challenging to carry out ultimately [21]. Large amounts of rhenium in the intermediate state result in low recovery efficiency of Re from leaching solution. Only by continuously improving the potential of the leaching system can the inexpensive rhenium ions be converted to their more expensive state, such as ReO_4^-. However, improving the potential of the leaching system can also accelerate the formation of the impeded dissolution layer on the surface of superalloy scrap. The leaching process finally conflicts between the leaching system potential and recovery rates of strategic metals from superalloy scrap.

Many researchers have introduced ultrasound into the leaching process of complex insoluble minerals to increase the leaching rates [22,23]. During the ultrasonic-assisted leaching process, ultrasonic cavitation can efficiently impact the solid surface and accelerate the diffusion of the leaching solution into the solid interior, thus improving the leaching rates [24,25]. LI et al [26] found that the higher leaching efficiency in the ultrasonic-assisted leaching process was mainly ascribed to the unique cavitation action of the ultrasonic waves. The ultrasonic-assisted leaching process was not only practical but also environmentally friendly [27]. YAN et al [28] found that the leaching efficiency of all the valuable metals could increase by 10% during the ultrasonic leaching process. XUE et al [29] found that the leaching rate of nickel from nickel sulfide ore at 150 min leaching under ultrasonic-assisted leaching process could obtain the same leaching rate of 300 min leaching under conventional leaching process. ZHANG et al [30] found that during the ultrasonic cavitation, the formation of hydroxyl radical and hydrogen peroxide made Ce(III) in the leaching solution oxidize to Ce(IV) without any extra oxidant.

This work intends to provide a novel and practical method to realize the strategic metals recovery from superalloy scrap. An ultrasonic field was introduced into the leaching process of superalloy scrap, with HCl as the dissolving agent and H_2O_2 as the solubilizers. The purposes of this study were to improve the leaching rates of strategic metals from superalloy scrap and promote the oxidation reaction of strategic metals. The physical and chemical coupling leaching mechanism of strategic metals from superalloy scrap by ultrasonic-assisted leaching method was investigated by leaching experiments and ICP, SEM, XRD, XPS, and EPR analysis.

2 Experimental

2.1 Experimental materials

In this study, the superalloy scrap was from Institute of Metal Research, Chinese Academy of Sciences. The chemical compositions of the samples are presented in Table 1, which mainly contains multiple strategic metals such as Ni, Co, Cr, Al, W, Re, and Ta. The phase compositions of strategic metals in the superalloy are mainly composed of the γ phase and γ' phase. The strengthening γ' phase is mainly composed of Al and Ta. As for the γ phase, the matrix γ phase consists of Ni, Co, Cr, W, and Re. Reagents such as HCl and H_2O_2 with an analytical grade were obtained from Shenyang Xinhua Reagent Co., Ltd., China. The aqueous solutions used in all experiments were prepared with deionized water.

The morphology of superalloy scrap was analyzed, and the result is shown in Fig. 1. From Fig. 1, the morphology of the superalloy scrap presents a smooth surface with some particles

Table 1 Chemical compositions of superalloy used in this study (wt.%)

Co	Cr	Ta	W	Re	Al	Ni
7.6	6.9	6.6	5.3	3.1	6.2	Bal.

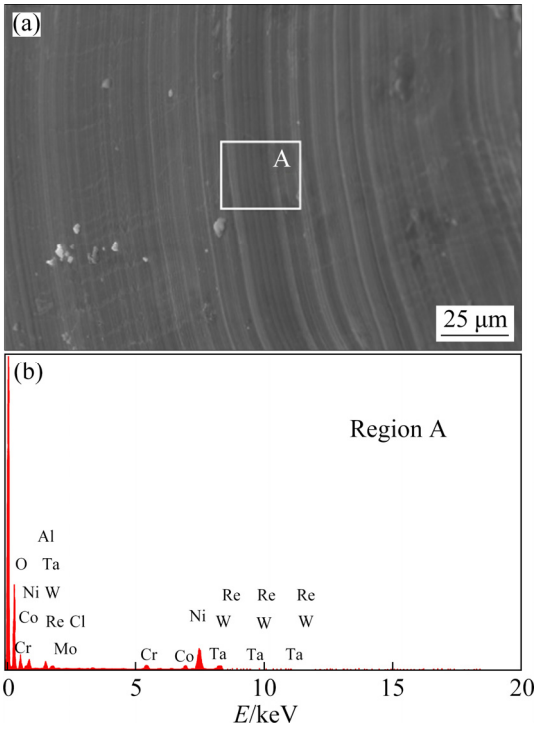

Fig. 1 SEM image (a) and EDS analysis (Region A) (b) of superalloy scrap

attached to the surfaces. The EDS results show that Region A consists of Ni, O, Al, Co, Cr, Mo, W, Ta, and Re. The EDS result of Region A (Table 2) is different from the original chemical compositions of the samples in the presence of O. Thus, it can be concluded that the sample surface is covered with an oxidation layer that inhibits the leaching process.

Table 2 EDS analysis results (Region A in Fig. 1) of superalloy scrap (wt.%)

O	Al	Cr	Ni	Co	Mo	Ta	W	Re
16.84	5.56	4.70	58.23	8.01	0.2	2.69	1.63	2.14

2.2 Experimental method

Figure 2 shows the schematic diagram of the leaching experiment device.

The ultrasonic-assisted leaching process of strategic metals from superalloy scrap was carried out in a thermostat-controlled ultrasonic bath with a power of 0−600 W (GT1022, Granbo Technology Industrial Shenzhen Co., Ltd., Shenzhen, China). The stirring speed was controlled by a frequency governor with a stirring speed of 0−1300 r/min (S212−90B, Hangzhou Yijie Technology Co., Ltd., China). The leaching experimental procedure was as follows. When the thermostat-controlled ultrasonic bath was heated to the desired temperature, the superalloy scrap with a specific concentration of HCl was placed into the thermostat-controlled ultrasonic bath. To hold back the decomposition of hydrogen peroxide at test temperature, the H_2O_2 was pumped into the flask at a specific rate during the leaching progress by a peristaltic pump

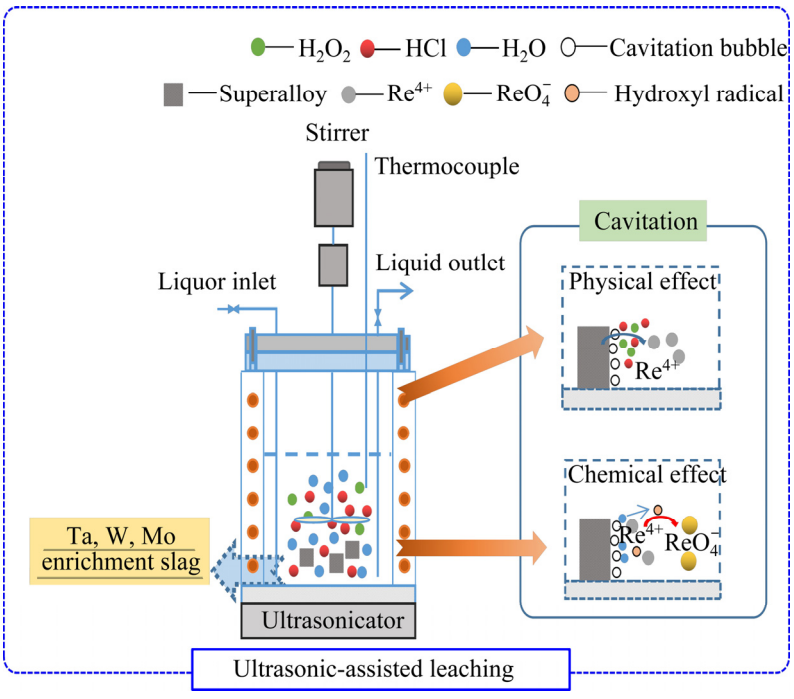

Fig. 2 Schematic diagram of leaching experiment device

(BT100S, Baoding Lead Fluid Technology Co., Ltd., China). After the leaching process, the conical flask was removed from the ultrasonic bath. To prevent the volatilization of hydrochloric acid at test temperature, all the leaching experiments were placed in a closed container. To avoid the emission of waste acid solutions, all the leaching experiments were conducted in the ventilated hood.

To determine the leaching performances of strategic metals from superalloy scrap, the experimental conditions were as follows: leaching time of 0−120 min, ultrasonic power of 200−600 W, HCl concentration of 8 mol/L, H_2O_2 content of 16 vol.%, stirring speed of 300 r/min, and leaching temperature of 80 °C.

To investigate the ultrasonic-assisted leaching mechanism of strategic metals from superalloy scrap, the experimental conditions were as follows: leaching time of 60 min, ultrasonic power of 0 and 600 W, HCl concentration of 8 mol/L, H_2O_2 content of 16 vol.%, stirring speed of 300 r/min, and leaching temperature of 80 °C.

To prove the existence of hydroxyl radicals in the ultrasonic-assisted leaching process, the EPR test was conducted under the same conditions as the ultrasonic-assisted leaching experiments.

2.3 Analytical methods

Chemical analysis of the superalloy scrap and the leaching solution was performed by ICP (Optima 8300DV, PE, USA). The leaching rates were calculated as follows:

$$\eta=c_1/c_2\times100\% \quad (1)$$

where η is the leaching rate of strategic metals from superalloy scrap, %; c_1 is the content of strategic metals in solution, wt.%; c_2 is the metal content in the initial superalloy scrap, wt.%.

SEM (Quanta 450, FEI, USA) was used to observe the morphologies of the superalloy scrap and leaching residues. XRD (PW3040/60, Philips, Netherlands) was used to investigate the phase composition of strategic metals in the leaching solution. The valence states of the strategic metals in the leaching solution were analyzed by XPS (Kratos Axis-ultra DLD, Japan). EPR (EMXnano, Bruker, Germany) was used to prove the existence of hydroxyl radicals in the ultrasonic-assisted leaching process.

3 Results and discussion

3.1 Leaching performance of strategic metals from superalloy scrap

3.1.1 Influence of leaching time and processes

Figure 3 presents the leaching rates of strategic metals from superalloy scrap, the SEM images and EDS analysis of leaching residues with different leaching time and processes.

With increasing time, the leaching rates of Re, Ni, Co, Al, and Cr increase linearly in different leaching processes, and W appears to be more minimally removed than other metals. For example, in the normal leaching process, when the leaching time is extended from 30 to 120 min, the leaching rates of Re, Ni, Co, Al, Cr, and W increase from 44.5%, 65.5%, 67.4%, 69.4%, 67.8%, and 19.2% to 86.4%, 90.7%, 92.4%, 95.1%, 98.4%, and 20.8%, respectively. The results indicate that leaching time plays an important role in strategic metals, especially Re leaching from superalloy scrap. For the ultrasonic-assisted leaching process, at a leaching time of 60 min, the leaching rates of Re, Ni, Co, Al, Cr, and W are 92.3%, 95.2%, 98.5%, 98.7%, 97.5%, and 27.2%, respectively. When the leaching time exceeds 60 min, the leaching rates of Re, Ni, Co, Al, Cr, and W are not further elevated. At a leaching time of 120 min, the leaching rates of Re, Ni, Co, Al, Cr, and W are only 6.8%, 0.5%, 1.4%, 1.2%, 2.3%, and 1.0% higher than those obtained at a leaching time of 60 min. The ultrasonic-assisted leaching process is completed at a leaching time of 60 min, indicating that ultrasonic treatment can effectively improve the leaching performance.

In addition, SEM and EDS analyses of the leaching residues at different leaching time were conducted, and the results are shown in Fig. 3 and Table 3. After the normal leaching for 30 min, compared with the surface of the initial superalloy scrap, the surface of the leaching residue is full of cracks with extensive particles of material attached, as shown in Fig. 3(a). The EDS analysis results of Region A show that the surface of the superalloy scrap is mainly composed of O, Al, Cl, Cr, Ni, Co, Mo, Ta, W, Re, etc. At a leaching time of 60 min, the surface of the superalloy scrap is entirely covered by particles. The EDS analysis results of Region B show that the particle is mainly composed

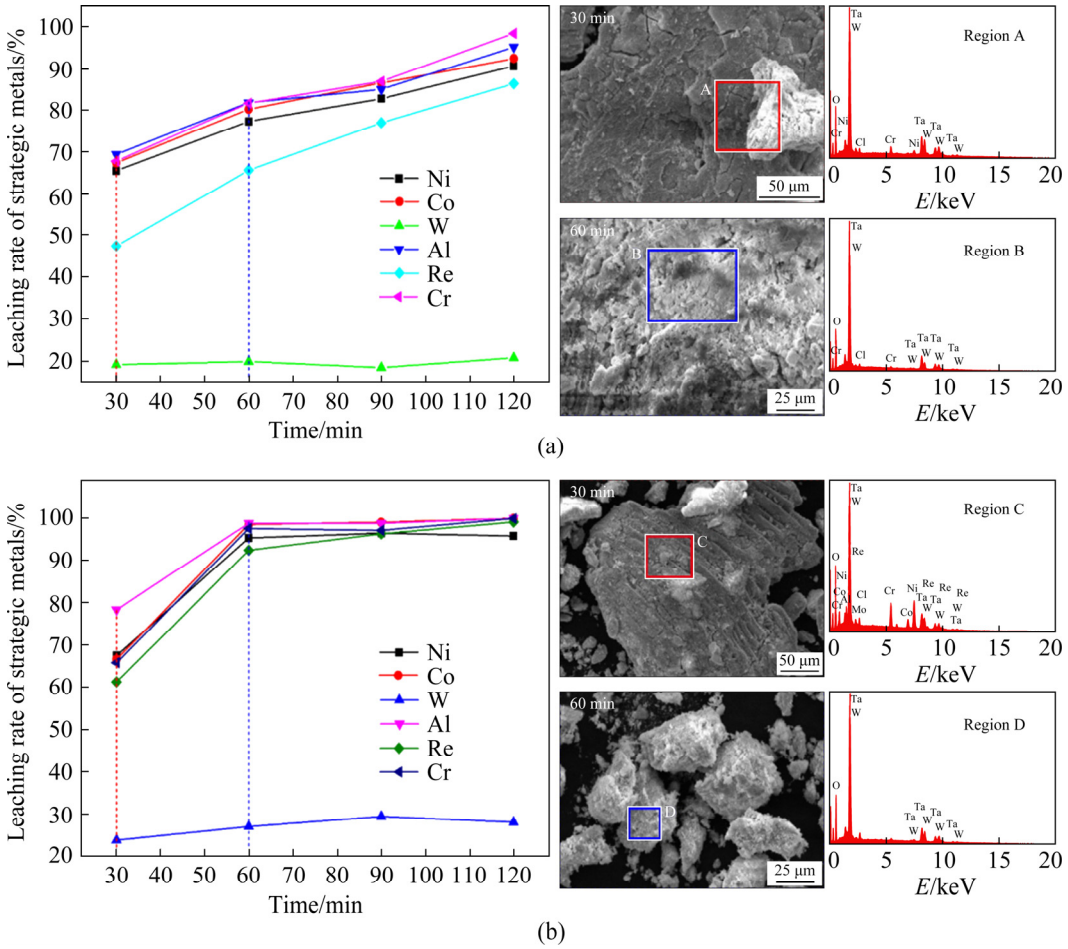

Fig. 3 Leaching rates of strategic metals from superalloy scrap, SEM images and EDS analysis of leaching residues at different time with different leaching processes: (a) Normal leaching; (b) Ultrasonic-assisted leaching

Table 3 EDS analysis results (Regions A, B, C and D in Fig. 3) of leaching residues at different leaching time (wt.%)

Region	O	Al	Cl	Cr	Ni	Co	Mo	Ta	W	Re
A	18.63	1.21	1.23	6.74	11.26	2.16	4.04	34.23	15.24	5.26
B	23.04	–	1.12	0.84	–	–	–	50.39	24.61	–
C	17.29	1.39	1.25	6.49	14.69	3.88	1.84	27.62	20.75	4.81
D	15.39	–	–	–	–	–	–	45.89	38.71	–

of O, Cl, Cr, Ta, W, etc. The enrichment of O, Cr, Ta, and W at the superalloy scrap surface indicates that an impeded dissolution layer has already been formed on the surface of the superalloy scrap, resulting in a low leaching efficiency of strategic metal from the superalloy scrap.

In the ultrasonic-assisted leaching process, at 30 min, the superalloy scrap was broken into particles of various sizes. The original smooth surface structure has disappeared and exhibits obvious particle attachment, as shown in Fig. 3(b). The EDS analysis results of Region C show that the surface of the superalloy scrap is mainly composed of O, Al, Cl, Cr, Ni, Co, Mo, Ta, W, Re, etc. The surface of the superalloy scrap presents a specific enrichment of O, Cr, Ta, and W, which results in identical leaching efficiency to the normal leaching process. At a leaching time of 60 min, the superalloy scrap collapses entirely into particles. The EDS analysis results of Region D show that the particles are only composed of O, Ta, W, etc. Combined with the leaching efficiency results, the ultrasonic-assisted leaching process of strategic metals from superalloy scrap was completed after

60 min. The ultrasonic-assisted leaching process can effectively improve the leaching rates of strategic metals from superalloy scrap by effectively removing the enrichment of O, Cr, Ta, and W on the surface of the superalloy.

3.1.2 Influence of ultrasonic power

To examine the leaching performances at different ultrasonic powers, a series of experiments were conducted. The results are shown in Fig. 4.

As shown in Fig. 4, ultrasonic power can dramatically affect the recovery of strategic metals from superalloy scrap. Within 60 min at 200 W of ultrasonic power, the leaching rates of Re, Ni, Co, Al, Cr, and W are only 76.4%, 80.5%, 81.9%, 83.9%, 83.2%, and 25.7%, respectively, while at 600 W, the leaching rates of Re, Ni, Co, Al, Cr, and W are 92.3%, 95.2%, 98.5%, 98.7%, 97.5%, and 27.2%, respectively. The results indicate that ultrasonic-assisted leaching can improve the leaching rates of Re, Ni, Co, Al, and Cr by approximately 15%. The SEM images show that at an ultrasonic power of 200 W, the surface of the superalloy exhibits apparent corrosion phenomena. The EDS analysis results of Region A indicate that the surface of the superalloy scrap exhibits apparent enrichment of O, Ta, and W. At an ultrasonic power of 600 W, the superalloy has wholly collapsed into particles. The EDS analysis results of Region B show that the particle is only composed of O, Ta, W, etc (Table 4), which indicates that the leaching process is thoroughly carried out. By increasing the ultrasonic power, ultrasonic cavitation can more effectively facilitate the leaching process of strategic metal from superalloy scrap, resulting in higher leaching rates of Re, Ni, Co, Al, Cr, and W.

3.2 Leaching mechanism of strategic metals from superalloy scrap

To better elucidate the leaching mechanism of strategic metals from superalloy scrap, samples with a working area of approximately 100 mm^2 were used in the leaching experiments. The morphologies of the superalloy scrap with various leaching processes are shown in Fig. 5.

In Fig. 5(a), it is worth noting that at a leaching time of 60 min, the residues present a denser structure in the normal leaching process, which prevents the leaching acid from diffusing into the interior to react with the unreacted sample. Region A consists of O, Al, Cr, Ni, Co, Ta, W, and Re. Compared with the original chemical composition of superalloy scrap, a higher amount of O, Ta, and W is retained in the impeded dissolution layer on the leaching residues after the normal leaching process. The structures of the impeded dissolution layer of the leaching residues contribute to the low leaching rates of strategic metals from superalloy scrap.

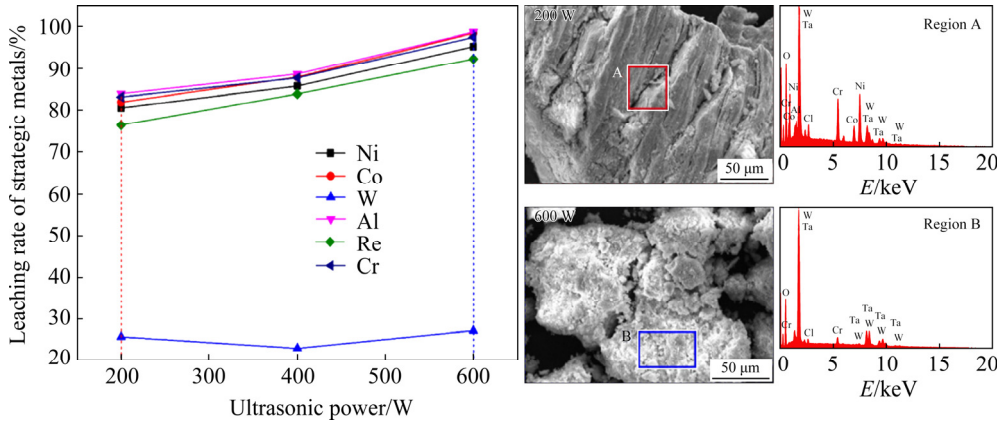

Fig. 4 Leaching rates of strategic metals from superalloy scrap, SEM images and EDS analysis of leaching residues at various ultrasonic powers in ultrasonic-assisted leaching

Table 4 EDS analysis results (Region A and B in Fig. 4) of leaching residues at various ultrasonic powers in ultrasonic-assisted leaching (wt.%)

Region	O	Al	Cl	Cr	Ni	Co	Mo	Ta	W	Re
A	18.63	1.21	1.23	6.74	11.26	2.16	4.04	34.23	15.24	5.26
B	15.39	–	–	–	–	–	–	45.89	38.71	–

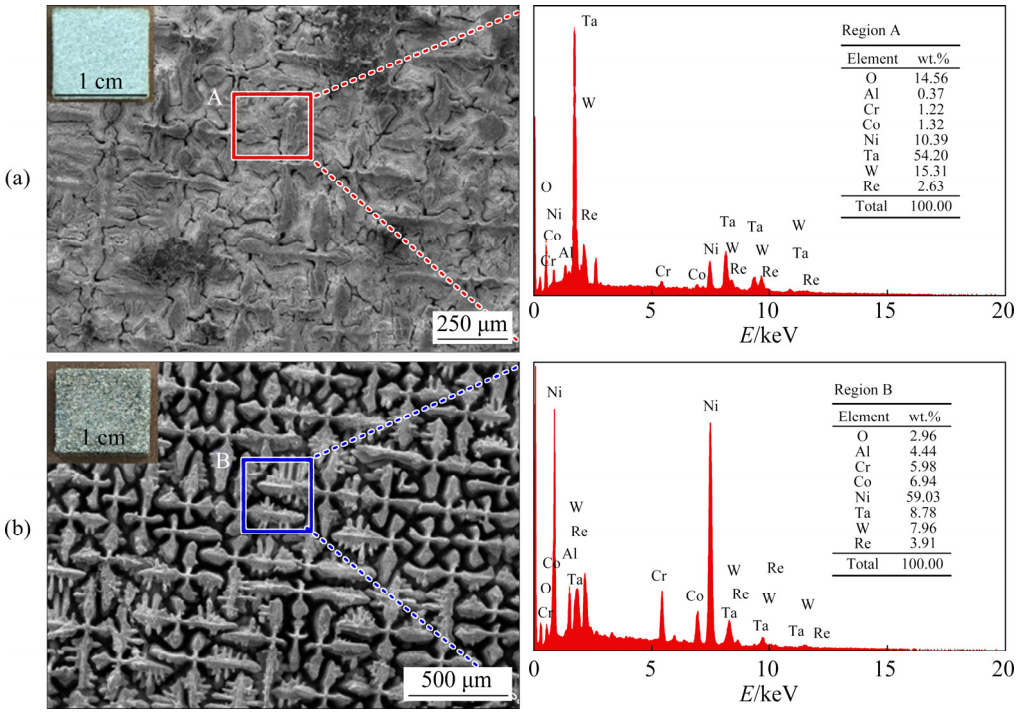

Fig. 5 SEM images and EDS analysis results of superalloy scrap by normal (a) and ultrasonic-assisted (b) leaching process

In Fig. 5(b), the surface of the residues obtained in the ultrasonic-assisted leaching process shows a relatively intact dendritic structure. The interdendritic structure disappears entirely, which demonstrates that the residues are further eroded without the formation of the impeded dissolution layer after the ultrasonic-assisted leaching process. In addition, the EDS results in Fig. 5(b) show that Region B consists of O, Al, Cr, Ni, Co, Ta, W, and Re. The amount of O, Ta, and W is considerably lower in the ultrasonic-assisted leaching residues than that in the normal leaching. A significant amount of Ta and W products are more thoroughly removed from the superalloy surface during the ultrasonic-assisted leaching process.

During the ultrasonic-assisted leaching process, a large number of cavitation nuclei are formed at the liquid−solid contact interface. With the explosion of cavitation nuclei, microjets with a velocity of 80−120 m/s are generated. Such microjets form a large impact force at the liquid−solid interface and trigger a strong mechanical stirring mechanism of ultrasonic [28,29]. The physical effect of ultrasonic cavitation continuously makes damage on the superalloy scrap surface by a high-speed collision between the superalloy and the leaching solution, which can remove the impeded dissolution layer, increase the contact interface with leached liquid, and finally promote the leaching rates of strategic metals from superalloy scrap.

Figure 6 shows the XRD patterns of leaching solutions after different leaching processes. From Fig. 6(a), the XRD patterns show that in the normal leaching process the leaching solution mainly consists of $ReCl_4$, $ReCl_5$, $NiCl_2$, $CoCl_2$, $CrCl_3$, and $AlCl_3$, which confirms that Re exists as Re(IV) and Re(V) in the leaching solution. However, in Fig. 6(b), the leaching solution mainly consists of $HReO_4$, $ReCl_4$, $NiCl_2$, $CoCl_2$, $CrCl_3$, and $AlCl_3$ in the ultrasonic-assisted leaching process.

The leaching reactions of Re in the leaching system mainly consist of multiple reaction processes (Table 5). The existence of Re(VII) verifies that the redox reactions of Re in the leaching system are enhanced in ultrasonic-assisted leaching process.

Figure 7 shows the valence distribution of Re in the leaching solution by normal and ultrasonic-assisted leaching processes. From Fig. 7(a), in the normal leaching solution, ReO_4^- exists only in the limited amounts of 1.88 wt.%, while after the ultrasonic-assisted leaching process, the content of ReO_4^- is approximately 56.24 wt.% (Fig. 7(b)). The increase in the content of ReO_4^- indicates that the

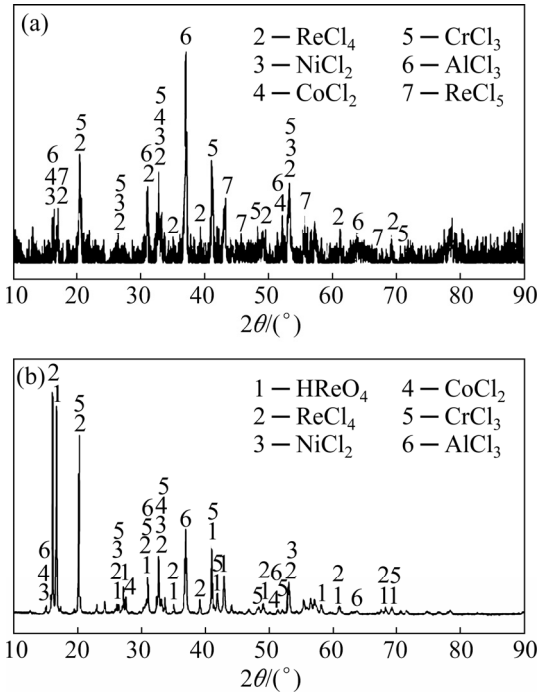

Fig. 6 XRD patterns of leaching solutions by normal (a) and ultrasonic-assisted (b) leaching

Table 5 Leaching reactions of Re in leaching system

Leaching reaction	Standard potential/V
$Re^{3+}+3e=Re$	+0.30
$ReO_2+4H^++4e=Re+2H_2O$	+0.26
$ReO_4^-+8H^++7e=Re+4H_2O$	+0.37

oxidation reaction is more complete, which is mainly attributed to two reasons. One of the reasons is the physical effect of ultrasonic cavitation which promotes the contact and reaction between the H_2O_2 and superalloy scrap, thereby enhancing the oxidation reaction of Re into ReO_4^-; Another reason may be the chemical effect of ultrasonic cavitation promoting the oxidation reaction of Re into ReO_4^-.

During ultrasonic cavitation, with the explosion of the cavitation nucleus, a local high-temperature and high-pressure environments of approximately 3000−6000 K and 30−100 MPa can be generated to form local “hot spots” [31,32]. These hot spots caused by ultrasonic cavitation can contribute to the disintegration of water to generate the H· and ·OH. The H· rapidly reacts with O_2 to form HO_2·, and the HO_2· disappears by the bimolecular reaction [33]. The related equations can be expressed as follows:

$$H_2O \xrightarrow{\text{Ultrasound}} H\cdot+\cdot OH \quad (2)$$

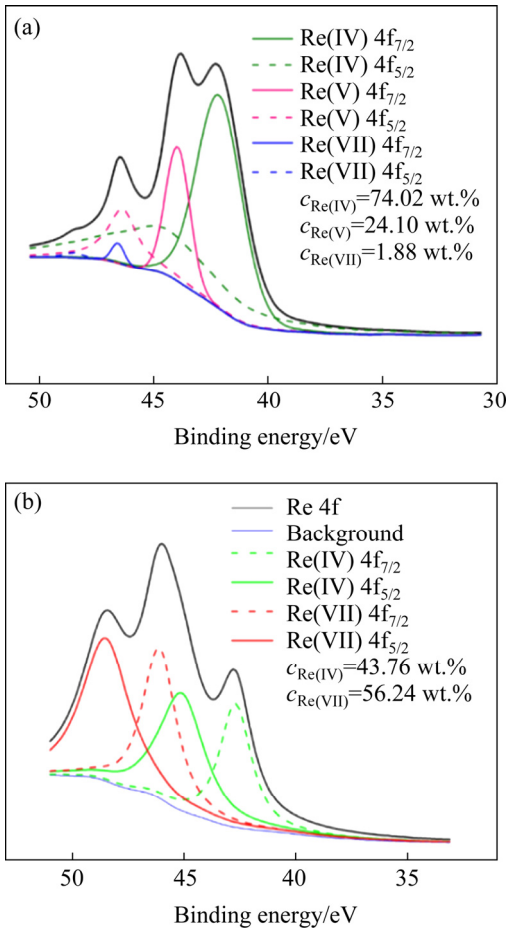

Fig. 7 XPS analysis results of leaching solution by normal (a) and ultrasonic-assisted (b) leaching

$$H\cdot+O_2 \longrightarrow HO_2\cdot \quad (3)$$

$$2HO_2\cdot \longrightarrow H_2O_2+O_2 \quad (4)$$

Based on the rates of Reactions (2) and (3), the H· and HO_2· speedily disappear in the system before reacting with DMPO. In contrast, the ·OH can react with DMPO and be alone detected. The EPR spectra in the ultrasonic-assisted leaching process is shown in Fig. 8.

From Fig. 8, in the HCl−H_2O_2 system with the ultrasonic-assisted leaching time of 0 min, only a signal of the noise of the measurement system can be observed. At 5 min in the HCl−H_2O_2 system, a quartet signal with the intensity ratio of 1:2:2:1 appears in the ultrasonic-assisted leaching, which is the characteristic spectrum of typical hydroxyl radical. With the extension of ultrasonic-assisted leaching time, the intensity of the signal peak of typical hydroxyl radical increases gradually. After the ultrasonic-assisted leaching time of 30 min, the intensity of the signal peak is no longer varied,

which indicates that the hydroxyl radical in the $HCl-H_2O_2$ system with the action of ultrasonic-assisted maintains a stable strength.

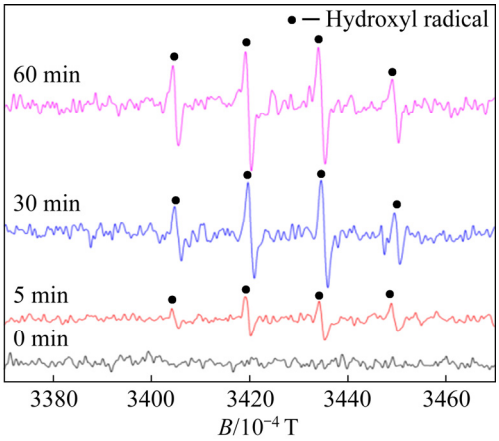

Fig. 8 EPR spectra for hydroxyl radical determination in $HCl-H_2O_2$ system at different leaching time in ultrasonic-assisted leaching process

Based on the standard potential of ·OH (2.33 V), the local potential of the leaching system can be significantly facilitated. The ·OH can contribute to the acceleration of the redox reaction of Re to ReO_4^- in the leaching system, which is consistent with the experimental results in Figs. 6 and 7. The results of the EPR test prove the existence of hydroxyl radicals in the $HCl-H_2O_2$ system with the action of an ultrasonic-assisted process, which promotes the oxidation reaction of Re into ReO_4^-.

In conclusion, ultrasonic cavitation can promote the contact and reaction between the $HCl-H_2O_2$ and superalloy scrap to improve the leaching rates of strategic metals from superalloy scrap by the physical effect of ultrasonic cavitation. At the same time, the chemical effect of ultrasonic cavitation can promote the production of hydroxyl radicals and result in stimulation of the chemical oxidation process of Re to ReO_4^-.

4 Conclusions

(1) The ultrasonic-assisted leaching process can obtain a higher leaching performance in a shorter leaching time. The economic leaching rates of Re, Ni, Co, Al, Cr, and W are 92.3%, 95.2%, 98.5%, 98.7%, 97.5%, and 27.2%, respectively, at a leaching time of 60 min, HCl concentration of 8 mol/L, H_2O_2 content of 16 vol.%, stirring speed of 300 r/min, and leaching temperature of 80 °C.

(2) The physical effect of ultrasonic cavitation continuously makes damage on the superalloy scrap surface by a high-speed collision between the superalloy and the leaching solution, which can remove the impeded dissolution layer, increase the contact area with leached liquid, and finally promote the leaching rates of strategic metals from superalloy scrap.

(3) Regarding the chemical effect, the ultrasonic cavitation can generate the disintegration of water, which produces oxidizing agents, such as ·OH and H_2O_2. Hydroxyl radicals significantly facilitate the potential of the leaching system and finally contribute to the acceleration of the redox reaction of Re to ReO_4^- in the leaching system.

Acknowledgments

The authors are grateful for the financial supports from the Chinese Academy of Sciences, China (No. E055A101), the Science and Technology Project of Shen-Fu Reform and innovation Demonstration Zone, China (No. 2021JH15), and the National Natural Science Foundation of China (No. U1710257)

References

[1] WANG Kai-meng, JING Hong-yang, XU Lian-yong, ZHAO Lei, HAN Yong-dian, LI Hai-zhou, SONG Kai. Microstructure evolution of 55Ni−23Cr−13Co nickel-based superalloy during high-temperature cyclic deformation [J]. Transactions of Nonferrous Metals Society of China, 2021, 31(11): 3452−3468.

[2] WANG Guang-lei, LIU Jin-lai, LIU Ji-de, ZHOU Yi-zhou, SUN Xu-dong, ZHANG Hai-feng, SUN Xiao-feng. Effect of orientation on stress-rupture property and related deformation microstructure of a Ni-base re-containing single-crystal superalloy at 900 °C [J]. Acta Metallurgica Sinica (English Letters), 2021, 34: 719−728.

[3] SHI Zhen-xue, LI Jia-rong, LIU Shi-zhong, WANG Xiao-guang, YUE Xiao-dai. Effect of Ru on stress rupture properties of nickel-based single crystal superalloy at high temperature [J]. Nonferrous Metals Science and Engineering, 2012, 22(9): 2106−2111.

[4] KIM M S, LEE J C, PARK H S, JUN M J, KIM, B S. A multistep leaching of nickel-based superalloy scrap for selective dissolution of its constituent metals in hydrochloric acid solutions [J]. Hydrometallurgy, 2018, 176: 235−242.

[5] TIAN Qing-hua, GAN Xiang-dong, YU Da-wei, CUI Fu-hui, GUO Xue-yi. One-step and selective extraction of nickel from nickel-based superalloy by molten zinc [J]. Transactions of Nonferrous Metals Society of China, 2021,

31(6): 1828−1841.

[6] WANG Long, ZHANG Ting-an, LV Guo-zhi, DOU Zhi-he, ZHANG Wei-guang, ZHANG Jing-zhong, NIU Li-ping, LIU yan. Carbochlorination of alumina and silica from high-alumina fly ash [J]. Minerals Engineering, 2019, 130: 85−91.

[7] YU Jin-jing, SUN Xiao-feng, LOU Jiang-xin, LANG Hai-xia. Recycled applications of a single crystal superalloy [J]. Advanced Materials Research, 2011, 239/240/241/242: 1422−1427.

[8] SRIVASTAVA R R, KIM M S, LEE J C, JHA M K, KIM B S. Resource recycling of superalloys and hydrometallurgical challenges [J]. Journal of Materials Science, 2014, 49: 4671−4686.

[9] YAGI R, OKABE T H. Continuous extraction of nickel from superalloy scraps using zinc circulation [J]. Metallurgical and Materials Transactions B, 2017, 48: 1494−1501.

[10] CUI Fu-hui, WANG Gang, YU Da-wei, GAN Xiang-dong, TIAN Qing-hua, GUO Xue-yi. Towards "zero waste" extraction of nickel from scrap nickel-based superalloy using magnesium [J]. Journal of Cleaner Production, 2020, 262: 121275.

[11] COOPER D R, SONG J W, GERARD R. Metal recovery during melting of extruded machining chips [J]. Journal of Cleaner Production, 2018, 200: 282−292.

[12] VIROLAINEN S, LAATIKAINEN M, SAINIO T. Ion exchange recovery of rhenium from industrially relevant sulfate solutions: Single column separations and modeling [J]. Hydrometallurgy, 2015, 158: 74−82.

[13] SRIVASTAVA R R, KIM M S, LEE J C. Novel aqueous processing of the reverted turbine-blade superalloy for rhenium recovery [J]. Industrial & Engineering Chemistry Research, 2016, 55: 8191−8199.

[14] XIANG Jun-yi, HUANG Qin-yun, LV Xue-wei, BAI Cheng-guang, Extraction of vanadium from converter slag by two-step sulfuric acid leaching process [J]. Journal of Cleaner Production, 2018, 170: 1089−1101.

[15] OLBRICH A, MEECE-MARKTSCHEFFEL J, JAHN M., ZERTANI R, STOLLER V, ERB M, HEINE K H, KUTZLER U. Recycling of superalloys with the aid of an alkali metal salt bath: US Patent, US20090255372A1 [P]. 2009−10−15.

[16] CHEN Xi-chun, SHI Cheng-bin, GUO Han-jie, WANG Fei, REN Hao, FENG Di. Investigation of oxide inclusions and primary carbonitrides in Inconel 718 superalloy refined through electroslag remelting process [J]. Metallurgical and Materials Transactions B, 2012, 43: 1596−1607.

[17] ZHOU Xue-jiao, CHEN Yong-li, YIN Jian-guo, XIA Wen-tang, YUAN Xiao-li, XIANG Xiao-yan. Leaching kinetics of cobalt from the scraps of spent aerospace magnetic materials [J]. Waste Management, 2018, 76: 663−670.

[18] FENG Rui-shu, XU Sheng-ming, LIU Jing, WANG Cheng-yan. The influence of Cl on the electrochemical dissolution of cobalt white alloy containing high silicon in a sulfuric acid solution [J]. Hydrometallurgy, 2014, 142: 12−22.

[19] WANG Long, WANG Shi-yang, SONG Zeng-yi, SUN Yuan, ZHOU Yi-zhou, PEI Xiao-yao, ZHANG Hong-yu. Electro-chemical dissolution behaviors of scrap superalloys in different electrolytes [J]. JOM, 2021, 73: 1978−1986.

[20] FERNANDES S Z, MEHENDALES S G, VENKATACHAKAM. Influence of frequency of alternating current on the electrochemical dissolution of mild steel and nickel [J]. Journal of Applied Electrochemistry, 1980, 10: 649−654.

[21] CHEN Chang-jun. Study on leaching scheme of valuable metals from superalloy scrap [D]. Lanzhou: Lanzhou University of Technology, 2020. (in Chinese)

[22] DOCHE M L, MANDROYAN A, MOURAD-MAHMOUD M, MOUTARLIER V, HIHN J Y. An ultrasonic-assisted process for copper recovery in a des solvent: Leaching and re-deposition [J]. Chemical Engineering and Processing: Process Intensification, 2017, 40: 24−29.

[23] GUNGOREN C, BAKTARHAN Y, DEMIR I, OZKAN S G. Enhancement of galena-potassium ethyl xanthate flotation system by low power ultrasound [J]. Transactions of Nonferrous Metals Society of China, 2020, 30(4): 1102−1110.

[24] CANIZARES P, RODRIGO M A, VIEIRA DOS SANTOS E, MARTINEZ H. Treating soil-washing fluids polluted with oxyfluorfen by sono-electrolysis with diamond anodes [J]. Ultrasonics Sonochemistry, 2017, 34: 115−122.

[25] YANG Jin-hong, HE Li-hua, LIU Xu-heng, DING Wen-tao, SONG Yun-feng, ZHAO Zhong-wei. Comparative kinetic analysis of conventional and ultrasound-assisted leaching of scheelite by sodium carbonate [J]. Transactions of Nonferrous Metals Society of China, 2018, 28(4): 775−782.

[26] LI Li, ZHAI Long-yu, ZHANG Xiao-xiao, LU Jun, CHEN Ren-jie, FENG Wu, KHALIL A. Recovery of valuable metals from spent lithium-ion batteries by ultrasonic-assisted leaching process [J]. Journal of Power Sources, 2014, 262: 380−385.

[27] XIE Feng-chun, LI Hai-ying, MA Yang, LI Chun-cheng, CAI Ting-ting, HUANG Zhi-yuan, YUAN Gao-qing. The ultrasonically assisted metals recovery treatment of printed circuit board waste sludge by leaching separation [J]. Journal of Hazardous Materials, 2009, 170: 430−435.

[28] YAN Shu-xuan, SUN Cong-hao, ZHOU Tao, GAO Rui-chuan, XIE Hua-sheng. Ultrasonic-assisted leaching of valuable metals from spent lithium-ion batteries using organic additives [J]. Separation and Purification Technology, 2021, 257: 117930.

[29] XUE Juan-qin, LU Xi, DU Ye-wei, MAO Wei-bo, WANG Yu-jie, LI Jing-xian. Ultrasonic-assisted oxidation leaching of nickel sulfide concentrate [J]. Chinese Journal of Chemical Engineering, 2010, 18(6): 948−953.

[30] ZHANG Dong-liang, LI Mei, GAO Kai, LI Jian-fei, YAN Yu-jun, LIU Xing-yu. Physical and chemical mechanism underlying ultrasonically enhanced hydrochloric acid leaching of non-oxidative roasting of bastnaesite [J]. Ultrasonics Sonochemistry, 2017, 39: 774−781.

[31] MAMO S K, ELIE M, BARON M G, SIMONS A M, GONZALEZ-RODRIGUEZ J, GONZALEZ R. Leaching kinetics, separation, and recovery of rhenium and component metals from CMSX-4 superalloys using hydrometallurgical processes [J]. Separation and Purification Technology, 2018,

212: 150−160.

[32] HUANG C P, DONG C D, TANG Z H. Advanced chemical oxidation: Its present role and potential future in hazardous waste treatment [J]. Waste Management, 1993, 13: 361−377.

[33] MASAKI K, KAZUHIRO S, NAOMI S K, TOSHIKUNI Y. Kinetic model for formation of DMPO-OH in water under ultrasonic irradiation using EPR spin trapping method [J]. Research on Chemical Intermediates, 2012, 38: 2191−2204.

超声空化作用下高温合金废料中战略金属的浸出机理

王 龙[1]，孙 元[2,3]，王诗洋[2,3]，张廷安[1]，吕国志[1]

1. 东北大学 多金属共生矿生态化冶金教育部重点实验室，沈阳 110819；
2. 中国科学院 金属研究所，沈阳 110016；
3. 高温合金二次资源绿色综合利用联合创新实验室，沈阳 110016

摘 要：为提高高温合金废料中战略金属的回收效率，提出一种超声辅助浸出工艺。在超声辅助浸出过程中，浸出时间为 60 min 时，高温合金废料中 Re、Ni、Co、Al、Cr 和 W 的浸出率分别为 92.3%、95.2%、98.5%、98.7%、97.5%和 27.2%，明显优于常规浸出工艺中浸出时间为 120 min 时的浸出效率。高温合金废料中战略金属浸出效率的提高可归因于超声空化作用下产生的物理和化学协同作用。超声空化的物理作用可以阻止高温合金废料表面溶解层的形成，促进浸出液与高温合金废料接触，从而提高高温合金废料中战略金属的浸出率；而超声空化的化学作用可以促进 $HCl–H_2O_2$ 体系中羟基自由基的产生，从而增强浸出体系的电位，促进体系中 Re 向 ReO_4^-的氧化反应过程。

关键词：战略金属；高温合金废料；浸出；超声波辅助浸出；羟基自由基

(Edited by Bing YANG)